2013

Transport Pathway across HCAECS uncer convective condtitions and The role of apoptosis in LDL transport through HCAECS

Janpen Phupeerasupong
CUNY City College

Transport pathway across HCAECs under convective conditions

and

The role of apoptosis in LDL transport through HCAECs

Thesis

Submitted in partial fulfillment of
the requirement for the degree

Master of Engineering (Biomedical)

at

The city College of New York
Of the
City University of New York

by

Janpen Phupeerasupong
February 2013

Approved:

_____

Professor John M. Tarbell, Thesis Advisor

_____

Professor John M. Tarbell, Chairman
Department of Biomedical Engineerin

Abstract

Advisor: John M. Tarbell

Previously, our lab has used an in vitro model consisting of Bovine Artery Endothelial Cells (BAEC) plated onto porous, polyester filters to measure the fluxes of water and LDL through BAEC monolayers [1]. The results showed that the leaky junction is the primary pathway for LDL transport under convective conditions, accounting for more than 90% of the transport and water was transported mostly through the break in the tight junction (77.7%). Later, BAEC monolayers were induced to undergo apoptosis with tumor necrosis factor alpha and cycloheximide (TNF α/CHX). The results showed that inhibiting apoptosis rate by Z-VAD-FMK can reduce permeability of BAEC monolayers under convective conditions. The results also showed that the rate of LDL transport across BAECs was proportional to the apoptosis rate [2].

In this study, the same 3-pore model was used to examine the contribution of vesicles, paracellular transport through breaks in the tight junction, and leaky junctions in solute and fluid transport through Human Coronary Artery Endothelial Cells (HCAEC). A 3-pore model indicated that water transports through both breaks in (61.5%) and leaky junctions (38.5%). Leaky junction carries most of the LDL and dextran (95.4 and 95.5%).

To examine the ability of Z-VAD-FMK and Q-VD-OPh in inhibiting apoptosis and reducing the permeability of HCAEC under convective conditions, TNFα/CHX was used to induce an elevated rate of apoptosis in HCAEC monolayers, convective fluxes of LDL and water were measured in the same way as BAECs. Then increases in apoptosis and permeability were reduced by treatment with the caspase inhibitor Z-VAD-FMK and

Q-VD-OPh. A strong correlation in the same way as BAECs between the rate of apoptosis and permeability was found only in Z-VAD-FMK.

Acknowledgements

First I would like to thank Limary Cancel for the time she has dedicated to me for through these years during my time in the lab. Her instructions and suggestions have been very valuable to me. Also my mentor, John M. Tarbell, for his support and knowledge. I also would like to thank everyone in the lab for the friendship and support. And last, I would like to thank my family for their love and encouragement.

Table of contents

List of Tables

List of Figures

I. Specific Aims

Atherosclerosis is the chronic inflammation of blood vessels. The affected arteries become thickened and irregular, resulting in the narrowing of the inner arterial channels, decreased blood flow and diminished oxygen supply to target organs. Atherosclerosis causes nearly 75% of cardiovascular related deaths and is found in 80 - 90% of Americans over the age of 30. Fat, cholesterol, calcium, and other substances form plaque, which builds up in arteries, hard plaque, narrowing the passage that blood flows through. That causes arteries to become hard and inflexible. It leads to cardiovascular disease, which is the leading cause of death in people over 45 years old.

Exactly how atherosclerosis begins or what causes it is still unknown. Many scientists think atherosclerosis starts because the innermost layer of the artery becomes damaged. This layer is called the endothelium. One of the causes of damage to the arterial wall is elevated levels of low density lipoprotein (LDL) in the blood.

In a previous study, our lab used an *in vitro* model consisting of BAEC monolayers plated onto porous, polyester filters to measure the fluxes of water and LDL through BAEC monolayers [2]. The results of that study showed that inhibiting apoptosis rate by Z-VAD-FMK can reduce permeability of BAEC monolayers under convective conditions. The results also showed that the rate of LDL transport across the endothelium was proportional to the apoptosis rate.

In the present study we propose to use a human cell *in vitro* model consisting of human coronary artery endothelial cell (HCAEC) monlolayers to monitor LDL transport

under convective conditions and assess the potential for reducing LDL permeability by reducing the rates of apoptosis.

Specific aims of the proposed research are

1) To examine the contribution of vesicles, paracellular transport through breaks in the tight junction, and leaky junctions in solute and fluid transport through HCAEC monolayers. We will measure water, dextran and LDL fluxes across HCAEC monolayers *in vitro* and use a 3-pore model to determine the relative contributions of vesicles, paracellular transport through breaks in the tight junction and leaky junctions associated with dying cells.

2) To test the hypothesis that inhibiting apoptosis can reduce the permeability of HCAEC in the same manner as BAEC under convective conditions. We will measure the rate of apoptosis in HCAEC monolayers *in vitro*. We will increase and reduce the rate of apoptosis using TNFα/CHX and two caspase inhibitors (Z-VAD-FMK and Q-VD-OPh), respectively, and measure the effect of these manipulations on the permeability of LDL under pressure.

Chapter 1: Introduction

I. Background and Significance

While there are many factors associated with the development of cardiovascular disease, the one that has attracted the greatest attention is diet and the level of blood serum cholesterol. Statins are the most common cholesterol medication; they work by reducing blood cholesterol levels. But fluid dynamical studies have shown that the regions of low shear and possible flow separation correlate with the pattern of naturally occurring lesion formation. In diet induced lesion in rabbits, Schwenke and Carew showed that the focal regions of elevated LDL concentration distal to flow bifurcations corresponded to regions of increased LDL degradation [3,4]. These lesion prone areas have recently been demonstrated to correspond to regions of increased density of cellular level leakage sites for macromolecules. These findings suggest that enhancing endothelial permeability to LDL is a primary risk factor for lesion localization [5]. Building on our previous work in BAECs [1,2], the aims of the proposed research take the next step towards the possibility of developing drugs that reduce endothelial permeability to LDL by confirming the relationship between apoptosis and permeability in a human *in vitro* model.

II. Low Density Lipoproteins (LDL)

Low density lipoproteins (LDL) are the major carriers of cholesterol in the bloodstream and play important role in the development of cardiovascular diseases. The LDL macromolecule is composed of a hydrophobic core of triglyceride and cholesterol,

surrounded by phospholipid, cholesterol esters, and protein. The protein consists of two structurally similar units, known as apoprotein B. LDL particles are approximately 22 nm in diameter and have a mass of about 3 million daltons. Studies in the laboratories of Michael Brown and Joseph Goldstein demonstrated that the uptake of LDL by mammalian cells requires the binding of LDL to a specific cell surface receptor that is concentrated in clathrin-coated pits and internalized by endocytosis [6].

III. Endothelium

Endothelial cells line all blood vessels. The lining that they create is called the endothelium. They serve as regulators of transport, much like epithelial cells. Molecules are transported across the endothelium in several ways. The tight junctions between cells permit the passage of molecules as large as 2 nm. Occasionally, leaky junctions are observed, and the junction permeability can be increased by agents that can cause vessels to dilate or constrict. These changes in permeability involve coordinated action of the cytoskeleton[7]. Macromolecules are also transported across endothelium by vesicles. This transport can occur in the fluid phase or by binding of macromolecules to receptors on the endothelial cell surface. Low molecular weight molecules can be transported by vesicles but the vesicular pathway accounts for a small fraction of the transport of water and of small solutes. Alteration in transport across endothelium by altering the permeability of arterial endothelium to protein is believed to be the treatment of atherosclerosis.

IV. Transport pathways

There are three primary transport pathways that molecules may take to travel from the vessel lumen to the subendothelial space [8].

IV.I Break in tight junction

When tight junctions are visualized under freeze-fracture electron microscopy, they are composed of a branching network of sealing strands. Each tight junction sealing strand is composed of a long row of transmembrane adhesion proteins embedded in each of the two interacting plasma membranes. The major transmembrane proteins in the tight junction are the claudins, which are essential for tight junction formation and function and differ in different tight junctions. A second major transmembrane protein in tight junctions is occludin. Claudins and occludins associate with intracellular peripheral membrane proteins called ZO proteins which anchor the strands to the actin cytoskeleton.

Figure 1.1 (adapted from [9]) is a conceptual model of the junction between endothelial cells. In this model, the cells are represented by two planes separated by a distance 2B (~20 nm). Tight junction is represented in the middle of the channel that are separated by an open slit of the width 2b (~1.5 nm). The break in the tight junction strand is an opening of width 2d (~150 nm).

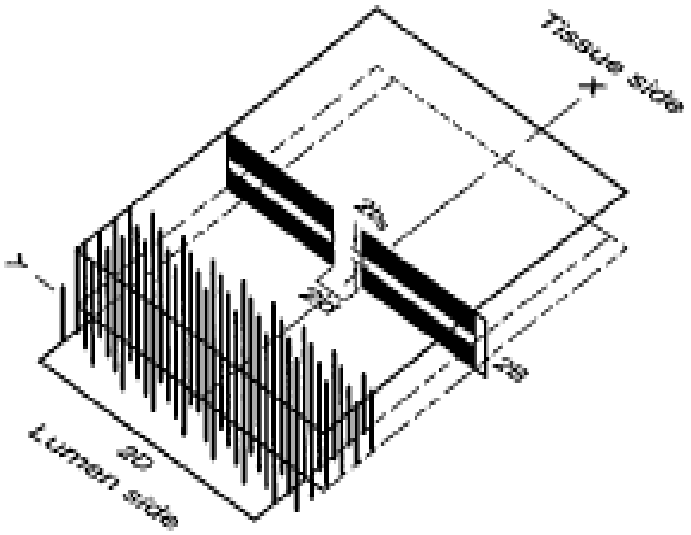

Figure 1.1 Three-dimensional sketch of a single periodic unit of width 2D, showing central orifice of height $2b_s$ in the junction strand. The break in the junction strand has width 2d.

The lumen side of the channel is filled with fiber matrix (bars perpendicular to the channel walls) representing the glycocalyx. The fibers are spaced 7 nm apart and have a radius of 0.6 nm. The model predicts that most of the water and larger solute (up to the size of albumin) flux pass through the breaks in the tight junction strand. The fiber matrix serves as the primary molecular filter. It has resistance to small solutes (< 1nm radius), but as the solute size increases to approach the fiber spacing, the resistance increases.

IV.II Leaky Junction

Normally, tight junctions would not allow significant passage of LDL even through breaks in tight junction because the widest part of the cleft is about almost the same size as LDL dimensions. Weinbaum et al. [10], building on earlier experiment observations by Gerrity et al. [11] proposed that the large pore was an infrequent, transiently leaky interendothelial cleft associated with a tiny fraction of cells that were in

the process of cell turn over i.e., either cell division or cell death. These cells had leaky junctions because they were either dying and being sloughed off by healthy neighboring cells or had poorly formed junctions because they were in the process of dividing. The dimension of the leaky junctions were estimated from HRP staining under electron microscopy to have a minimum width of 15 nm and a maximum width of 1000 nm around dying or dead cells [12].

IV.III Vesicles

Specific molecules such as LDL are often transported into cells through receptor-mediated endocytosis. The clathrin-mediated endocytic pathway plays an important role in the selective uptake of proteins at the plasma membrane of eukaryotic cells.

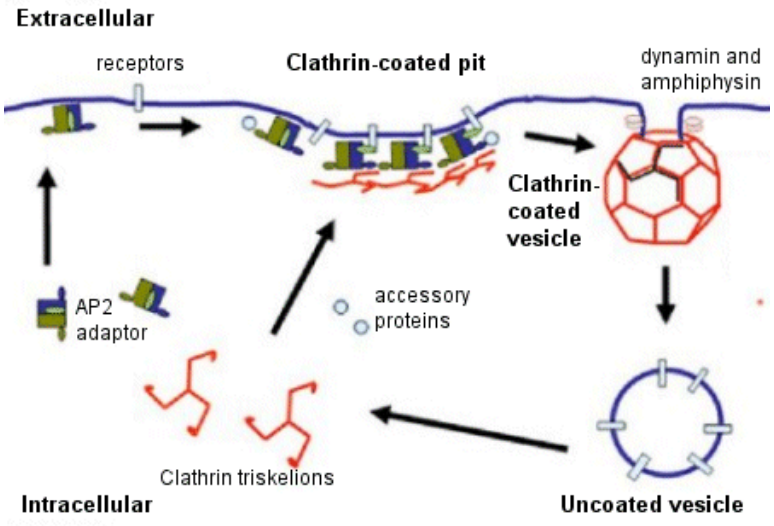

Figure 1.2 Outline of the main events in receptor-mediated endocytosis [13].

The process begins at the under-surface of the plasma membrane with the sequential assembly of coat components to form a clathrin-coated pit. Internalized

receptors interact with a class of molecules called adaptors and thus become clustered into the growing coated pit. The adaptors link the membrane proteins with the clathrin that forms the outer layer of the coat. Together with accessory and regulatory molecules, cargo proteins, adaptors and clathrin co-assemble, and the growing coated pit invaginates. In the final stage, the membrane neck is severed to form a closed coated vesicle[13]. (Figure 1.2)

V. Apoptosis

When cells are no longer needed, they commit suicide by activating an intracellular death program. This process is called "programmed cell death" or "apoptosis". The number of cells in multicellular organisms is regulated by this process. Cells that die as a result of acute injury typically swell and burst. They spill their contents all over their neighbors- a process called cell necrosis- causing a potentially damaging imflammatory response. By contrast, a cell that undergoes apoptosis dies neatly, without damaging its neighbors. The cell shrinks and condenses. The cytoskeleton collapses, the nuclear envelops disassembles, and the nuclear DNA breaks up into fragments. Most importantly, the cell surface is altered, displaying properties that cause the dying cell to be rapidly phagocytosed [14].

The intracellular machinery responsible for apoptosis seems to be similar in all animal cells. This machinery depends on a family of proteases that have a cysteine at their active site and cleave their target proteins at specific aspartic acids. They are therefore called "caspases". They are synthesized in the cell as inactive precursors or "procaspases" which are activated by cleavage at aspartic acids by other caspases [14].

Two main pathways leading to caspase activation have been characterized [15]. The extrinsic pathway is activated by ligand-bound death receptors of the tumor necrosis factor (TNF) receptor family [16] or Fas. Procaspases activation can be triggered from outside the cell by the activation of death receptors on the cell surface then aggregate procaspase-8 molecules, which cleave and activate one another. The activated caspase-8 molecules then activate the downstream procaspases to induce apoptosis. The intrinsic pathway happens when cells are damaged or stressed; they kill themselves by triggering procaspase aggretion and activation from within the cell, mitochondria are induced to release cytochrome c into cytosol, where it binds and activates an adaptor protein called Apaf-1, procaspase-9, and dATP to form a complex called the apoptosome [17]. This complex activates caspase 9, which then activates effector caspases to induce apoptosis. Death receptors can also activate the intrinsic pathway through cleavage of Bid [18].

The Bcl-2 family of intracellular proteins helps regulate the activation of procaspases. Some members of this family, like Bcl-2 itself or Bcl-X_L, inhibit apoptosis by blocking the release of cytochrome c. Another important family of intracellular apoptosis regulators is the IAP family. These proteins inhibit apoptosis in two ways: they bind to some procaspases to prevent their activation, and they bind to caspases to inhibit their activity.

VI. Endothelial Transport EQ

The equation for water flux across the endothelium is described by the equation describing membrane transport processes generated simultaneously by osmotic pressure and mechanical pressure [19]

$$J_v = L_p (\Delta P - \sigma \Delta\pi) \quad (1)$$

where J_v is the flux across the endothelium, L_p is the hydraulic conductivity, ΔP is the mechanical pressure differential across the endothelium, σ is the reflection coefficient and $\Delta\pi$ is the osmotic pressure differential.

Solute transport via diffusion and convection through a single pathway can be described using the following relationships [20]

$$P_e = P_0 Z + (1-\sigma) J_v \quad (2)$$

where P_0 is the diffusive per.meability, P_e is the apparent permeability and it has been assumed that the concentration in the abluminal side is much less than the lumen side. The relative importance of diffusion to convection is determined by Z, defined as

$$Z = N_{Pe}/[\exp(N_{Pe})-1] \quad (3)$$

where N_{Pe} is the Peclet number,

$$N_{Pe} = [(J_v)(1-\sigma)]/P_o \quad (4)$$

If we allow for vesicular transport that is strictly diffusive (i.e. no water flux through vesicles), and two convective pathways (a pathway through the breaks in the tight junction and a leaky junction pathway) then the following 3-pore model equations arise

$$J_v = J_{v2} + J_{v3} \quad (5)$$

$$P_e = P_{ov} + P_{o2} Z_2 + J_{v2}(1-\sigma_2) + P_{o3} Z_3 + J_{v3}(1-\sigma_3) \quad (6)$$

Jvi is the water flux through pore i ; Pov is the diffusive permeability of the vesicular pathway ; Poi is the diffusive permeability of pore i ; σ i is the reflection coefficient of pore i and Zi is defined by equations (3) and (4) with the appropriate subscripts for pore i.

This model will be used to determine the contribution of each pore to the overall water and LDL transport for control experiments.

Chapter 2 : Transport Pathway Across HCAECs under convective conditions

I. Introduction

In a previous study in our lab, Cancel et al. showed that the leaky junction associated with dying or dividing cells is the dominant pathway for LDL transport under convective conditions, accounting for more than 90% of the transport. The vesicular pathways accounted for the remainder (9.1%). Albumin was also preferentially transported through the leaky junction (44%) but had significant contributions from the break in the tight junction pathway (36%) and the vesicular pathway (20%). Water was transported mostly through the break in the tight junction (77.7%) with a portion going through the leaky junction (22.3%) [1].

The present study aims to similarly characterize the transport pathways of human coronary artery endothelial cells (HCAEC).

II. Materials and Methods

The following chemicals were obtained from Cell Applications, Inc (San Diego, CA): MesoEndo cell growth medium, basal endothelial cell medium, trypsin-EDTA solution, HBSS, and trypsin neutralizing solution. Dimethyl sulfoxide (DMSO), fibronectin and dextran 70kDa were from Sigma (St. Louis, MO). Untagged human LDL and fluorescent DiI-LDL were obtained from Biomedical Technologies (Stoughton, MA).

Cell culture. Human Coronary Artery Endothelial Cells were purchased from Cell Applications, Inc. (San Diego, CA). Cells were grown in T-75 flasks in MesoEndo complete cell growth medium and were kept at 37° C and 5% CO_2. The medium was replaced every 2-3 days. For the transport experiments, cell were plated on fibronectin-coated polycarbonate filter in Transwell supports at a density of $7.5x10^4$ cells/cm^2. Experiments were carried out on monolayers 6 days post plating.

Measurement of water and solute flux. An experimental apparatus was developed in our laboratory that could be used to measure both water flux and solute permeability across HCAEC monolayers. The HCAEC were sealed within the chamber (Polyethylene terephthalate, PET) to form luminal (top) volume that was completely isolated from the abluminal (bottom) volume. The luminal part was fed with a flow of gas (5% CO_2-95% balance air) to maintain the solution in contact with the cells at physiological pH of 7.4. The outlet from the PET chamber was attached to Tygon and borosilicate glass tubing and an abluminal liquid reservoir. When a 10-cm H_2O differential pressure was applied (by adjusting the height of the reservoir), the water flux (J_v) was measured by tracking the position of a bubble inserted in to the glass tube. The bubble displacement data were used to compute J_v values using

$$J_v = (\Delta d/\Delta t) \times F/A \qquad (7)$$

where $\Delta d/\Delta t$ is the bubble displacement per unit time, A is the area of the Transwell filter and F is a tube calibration factor.

The fluorescence intensity in the abluminal compartment was recorded and then converted to concentration by mean of a calibration curve and the permeability was calculated by

$$P_e, P_o = (\Delta C_a/\Delta t) \times V_a \times (1/C_1 A) \qquad (8)$$

where P_e (P_o) is the convection (diffusive) permeability, $\Delta C_a/\Delta t$ is the change in abluminal concentration with respect to time, V_a is the fluid volume in the abluminal compartment, C_1 is the concentration in the luminal compartment and A is the area of the filter.

Statistical analysis Permeability and water flux values were normalized with respect to control and presented as mean $\pm$ SEM. Data sets were analyzed for statistical significance by ANOVA and $p<0.05$ was considered statistically significant.

III. Results and discussion

Table 2.1 summarizes the water flux and permeability data for both LDL and dextran. Jv values are the average water fluxes measured for all monolayers in a set (LDL or dextran). P_o values are the permeabilities under diffusive conditions after sealing, P_e values are the apparent permeability coefficients that account for both diffusive and convective contributions during the application of 10-cm H_2O hydrostatic pressure differential. The Peclet numbers and osmotic reflection coefficients are based on the one pore model (Eqs.2-4)

Table 2.1 Summary of data from 10cmH_2O differential pressure solvent drag experiments

Macro molecule	J_v, cm/sx10^{-6}	P_o, cm/sx10^{-7}	P_e, cm/sx10^{-7}	Pe/Po	N_{Pe}	σ
LDL	5.25±0.52 n=7	2.44±0.39 n=28	27.59±3.22 n=24	11.31±2.24	11.31	0.47
Dextran	7.88±0.57 N=6	3.31±0.56 N=20	24.44±2.54 N=23	7.38±1.47	7.40	0.69

Values are mean±SEM. Reflection coefficient (σ) and Peclet number (N_{Pe}) values were computed based on the 1-pore model as described by Eqs. 2-4. Neither the diffusive permeability (P_o) or the apparent permeability coefficient (P_e) values for the LDL and dextran are statistically different from one another (P>0.19).

Comparing with previous BAEC experiments, LDL had $J_v = 5.88\pm0.63\text{x}10^{-6}$ cm/s, $P_o = 2.08\pm0.13\text{x}10^{-7}$ cm/s, $P_e = 13.16\pm3.64\text{x}10^{-7}$ cm/s. N_{Pe} and σ were calculated to be 6.36±0.51 and 0.768±0.017 respectively. Albumin had $J_v = 4.90\pm0.85\text{x}10^{-6}$ cm/s, $P_o = 32.10\pm3.50\text{x}10^{-7}$ cm/s, $P_e = 59.70\pm6.30\text{x}10^{-7}$ cm/s. N_{Pe} and σ were calculated to be 1.50±0.31 and 0.11±0.008 respectively. The LDL reflection coefficient is slightly lower and the N_{Pe} is slightly larger in HCAEC when compared to BAECs. For dextran, both the reflection coefficient and the N_{Pe} are much larger compared to the values calculated for albumin in BAECs. This could in part be explained by the fact that albumin can be transported in vesicular pathway but dextran can not.

Cell fixation and receptor blocking experiments

To examine the possible contribution of transcytosis in vesicles to total solute transport, we fixed the monolayers with 1% paraformaldehyde. The fixation prevents transcellular transport. By comparing permeability of fixed monolayer with control monolayers, the contribution of this pathway can be assessed. The results showed that fixation reduced the diffusive permeability 1.96 fold.

To test the role that LDL receptors play in transport across enthothelium, we ran experiments in which an excess of untagged native LDL was added to saturate the receptors. In these experiments, 10 μ g/ml Dil-LDL was added to one monolayer, and 10μg/ml Dil-LDL plus 500μg/ml untagged, native LDL was added to the other monolayer. The results showed that incubation with excess LDL reduced the diffusive permeability 1.90 fold which is very similar to the fixation experiments. So we combined the data from fixation experiments and receptor blocking experiments together (no significance between fixation and receptor blocking, $p>0.92$) and found that there is a significant difference in diffusive permeabilities ($p<0.015$) between control and test monolayers.

Based on average of fixation and receptor blocking experiments, the contribution of transcytosis in vesicles can be assessed.

$$P_{ov} = P_o - P_{o,\text{fixed/excess LDL}} \qquad (9)$$

Control monolayers had an average diffusive permeability (P_o) of $2.44\text{x}10^{-7}$ cm/s. The average diffusive permeability for fixed and excess LDL monolayers was $1.27\text{x}10^{-7}$ cm/s. The contribution of transcytosis in vesicles was computed (Eq.9) to be $1.17\text{x}10^{-7}$ cm/s.

3-pore model analysis

We first assumed that the vesicular pore (v) does not transport water. Pore 2 which represents the break in tight junction will only allow water and dextran because LDL is too large. Pore 3 is the leaky junction, allows water, dextran and LDL transport and is so large that the reflection coefficients for both dextran and LDL are zero. From our dextran and LDL transport data using the experimental apparatus, we have noticed

that P_e value of dextran and LDL are about the same ($p>0.44$), therefore, the average of the P_e values obtained for dextran and LDL were used. To complete specification of the problem, we assigned value of σ_2^d and solved the remaining parameters. The five equations had real solutions only for σ_2^d in the range of 0.97 to 0.99. Results are presented in Table 2.2 for $\sigma_2^d = 0.97$.

Table 2.2 Summary of 3-pore analysis, contribution of each pore to the overall solute permeability are given in the unit of cm/s x 10^{-6} (σ_2^d =0.97)

Component	Vesicle	Pore 2	Pore 3	Total
Water	-	3.97 (61.5%)	2.49 (38.5%)	6.46
Dextran	-	0.12 (4.6%)	2.48 (95.4%)	2.60
LDL	0.11 (4.5%)	-	2.49 (95.5%)	2.60

* J_{v3} was calculated from average of $P_{e\ LDL}$ and $P_{e\ dex.}$

Table 2.2 indicates that water transports through both pore 2 (61.5%) and pore 3 (38.5%); pore 3 carries most of the LDL and dextran. As in Fig 1.1, the model predicts that most of the water flow and solute flux up to the size of albumin can pass through the breaks in tight junction strands. The glycocalyx serves as the primary molecular sieve, which offers little resistance to small solutes, but as the solute size increases to approach the fiber spacing of 7 nm, the matrix resistance increases. A 70-kDa dextran, which is about the same size as albumin, was expected to have a large contribution from the break in tight junction strand. The inconsistent results of dextran transport pathway from Table 2.2 could be due to the denser glycocalyx in HCAECs compared to BAECs.

From the present study, we can see that water transport in HCAECs occurs through both the breaks in tight junction strand (61.5%) and leaky junctions (38.5%). This is similar to results previously obtained using BAECs [1], although the portion of water transported occurs through breaks in tight junction strand was larger in that study

(77.7%). The average P_o value of BAECs and HCAECs is not so different for LDL transport, but the average P_e and P_o values of dextran in HCAECs are a lot lower than that of albumin in BAECs despite the fact that dextran is slightly similar in size. This can be explained in part by the fact that dextran can not be transported by vesicular pathway like albumin. However, even taking into account the contribution of the vesicular pathway, the diffusive permeability of albumin is about 4 times larger than that of dextran. This leads to the calculation of a very large dextran refection coefficient (σ_2^d =0.97, Table 2.2) resulting in small portion of dextran (4.6%) being transported through breaks in tight junction strand (compare to albumin in BAECs: σ_2^a =0.49, 36% of transport through pore 2). The large reflection coefficient suggests a very dense glycocalyx, as mentioned before.

Another difference between BAECs and HCAECs is that only 4.5% of LDL molecules are transported through vesicular pathway in HCAECs (compared to 9.1% in BAECs). P_e for LDL in HCAECs is about 2 times larger than that in BAECs while P_o is about the same, as mentioned above. As we see in Chapter 3 (below) this could be explained by the fact that control HCAEC monolayers have an apoptosis rate that is more than six times that of control BAEC monolayers. The presence of more leaky junctions due to apoptosis could also explain why a larger portion of the water is transported through this pathway than in our previous study with BAECs.

Chapter 3: The role of apoptosis in LDL transport through HCAEC monolayers

I. Previous studies

In a previous study, Cancel et al. [2] increased the apoptosis rate of BAEC monolayers with TNFα/CHX. Treatment with TNFα/CHX induced a 18.3 fold increase on apoptosis and a 4.4 fold increase in LDL permeability. The increases in apoptosis and permeability were attenuated by treatment with the caspase inhibitor Z-VAD-FMK. Addition of Z-VAD-FMK attenuated the increase in permeability to 3.5 fold when 50μm Z-VAD-FMK was added, and to 2.2 fold when 100 μm Z-VAD-FMK was added. The correlation between the normalized LDL permeability and apoptosis rate had a Pearson Product Moment Correlation coefficient of 0.72 which shows a strong relationship between LDL permeability and apoptosis.

In the present study, we want to test the hypothesis that Z-VAD-FMK can inhibit apoptosis and hence reduce the permeability of HCAEC under convective condition as it did in BAEC monolayer in the previous study. Another caspase inhibitor, Q-VD-OPh will also be tested for its ability to reduce apoptosis and permeability of HCAEC. Q-VD-OPh is an irreversible caspase inhibitor that inhibits caspases 1, 3, 8, and 9. The advantage of Q-VD-OPh over Z-VAD-FMK is that it is non-toxic. A preliminary study showed no evidence of toxicity in mice injected with >1,000 mg/kg.

II. Materials and Methods

Cell culture Human Coronary Artery Endothelial Cells were purchased from Cell Applications, Inc. (San Diego, CA) and grown in MesoEndo complete cell growth medium, also from Cell Applications. Z-VAD-FMK was from EMD Chemicals (La Jolla,

CA); TNFα and cycloheximide were from Sigma (St. Louis, MO); Q-VD-OPh was obtained from SM Biochemicals LLC (Anaheim, CA). For transport experiments, cells were plated onto fibronectin-coated Transwell membranes (Corning, Acton, MA) at a density of $7.5x10^4$ cells/cm^2. Experiments were carried out on monolayers 6 days post plating.

Induction, Inhibition and measurement of Apoptosis HCAEC were incubated with tumor necrosis factor alpha (TNFα; 20 ng/mL) and cycloheximide (3 μg/mL) in growth medium for 3 hours and 20 minutes. To inhibit apoptosis, some monolayers were simultaneously treated with pan-caspase inhibitor Z-VAD-FMK at concentrations of 12.5 μg/mL or 25 μg/mL and Q-VD-OPh at concentrations of 50 μg/mL or 100 μg/mL. The inducer was then remove and the monolayer were allowed to recover for 20 hours in the presence or absence of the inhibitor.

We found that incubation with the inhibitors had to be continued during the measurement of LDL permeability, or a rapid cell death would occur. For this set of experiments, Z-VAD-FMK and Q-VD-OPh were added to the experimental media (1% BSA) for filters that had been induced to undergo apoptosis in the presence of the inhibitors. Control and TNFα/CHX-treated filters received the same dose of DMSO, which is the vehicle in which inhibitors were dissolved.

Apoptosis rates were determined using Vibrant Apoptosis assay kit#2 from Molecular Probes (Eugene, OR) per manufacturer's instructions. This assay uses the high affinity binding of annexin V to phosphatidylserine to identify apoptotic cells. Propidium iodine (PI) was used to identify necrotic cells. The apoptosis rate is define as the number

of apoptotic cells in a field divided by the total number of cells in the field, and presented as percent.

Measurement of solute and water flux The measurement of solute and water flux was done in the same manner as in Chapter 2.

Statistical analysis Permeability and water flux values were normalized with respect to control and presented as mean±SEM. Data sets were analyzed for statistical significance by ANOVA and $p<0.05$ was considered statistically significant.

III. Results and Discussion

Effect of TNF α/CHX and Z-VAD-FMK on apoptosis rate and LDL permeability

HCAEC monolayers were incubated with TNFα/CHX for 3 hours and 20 mins in the presence or absence of the inhibitor Z-VAD-FMK. The baseline apoptosis was 2.0 ± 0.249%. TNFα/CHX treated monolayers had an apoptosis rate of 9.1 ± 0.476%, a 4.5-fold increase over baseline. When the cells were treated with 12.5μM Z-VAD-FMK and 25μM Z-VAD-FMK, the apoptosis was significantly decreased to 1.59-fold and 2.05-fold, respectively (Fig. 3.1 A). Comparing to the study in BAECs [2], control monolayers had baseline apoptosis of only 0.3% (almost 7-fold higher in HCAECs) but when TNFα/CHX was added, apoptosis rate was dramatically raised to 18.3-fold over baseline. When BAECs were treated with 100 μM Z-VAD-FMK and 50 μM Z-VAD-FMK, the apoptosis was decreased to 6.0- and 10.0- fold times the baseline, respectively. Treatment with TNFα/CHX clearly had a bigger effect on apoptosis rates on BAECs, while addition

of Z-VAD-FMK showed similar effects on apoptosis rates for both BAECs and HCAECs. Note, however, that the apoptosis rate was still higher in TNFα/CHX-treated HCAEC monolayers (9.1%) than in similarly treated BAEC monolayers (5.9%).

Fig. 3.1 B shows the effect of TNFα/CHX and Z-VAD-FMK on the convective permeability (P_e) of HCAEC monolayers to LDL. Control monolayers had baseline P_e of $3.32x10^{-6} \pm 4.57x10^{-7}$ cm/s. The permeability was elevated by 3.40 fold with when treated with TNFα/CHX. Addition of Z-VAD-FMK significantly reduced the increase in permeability to 1.17 when 12.5μM Z-VAD-FMK was added and 0.79 when 25μM Z-VAD-FMK was added. BAECs had similar baseline P_e ($2.07x10^{-6} \pm 3.18x10^{-7}$ cm/s) and a similar increase with treatment with TNFα/CHX (4.4-fold). In BAECs, addition of Z-VAD-FMK significantly decreased the permeability to 2.2-fold when 100 μM Z-VAD-FMK was added and 3.5-fold when 50 μM Z-VAD-FMK was added [2].

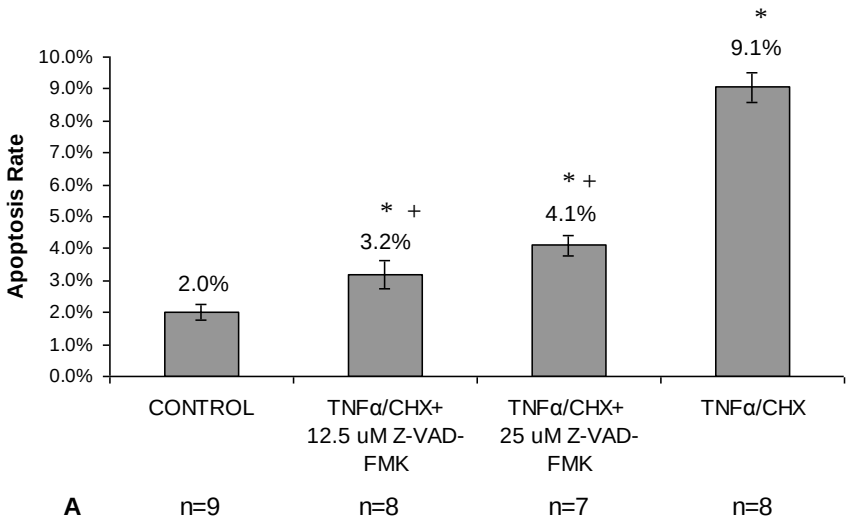

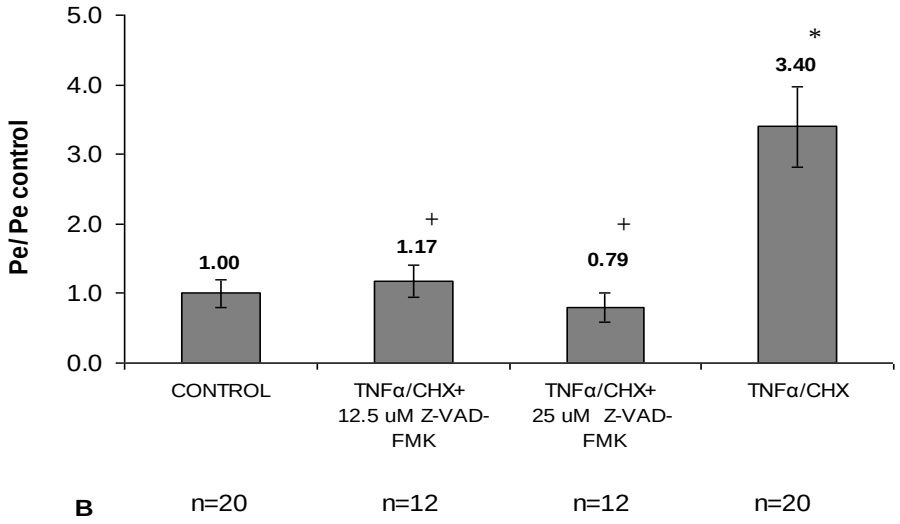

Fig 3.1 Effect of TNFα/CHX and Z-VAD-FMK on (A) apoptosis rate (B) convective permeability on HCAEC monolayer. Control monolayers had an average P_e of $3.32x10^{-6} \pm 4.57x10^{-7}$ cm/s. Mean±SEM shown. *p< 0.0032 vs. control, +p< 0.0013 vs. TNFα/CHX.

Effect of TNFα/CHX and Z-VAD-FMK on water flux

The water flux of treated monolayers was measured to assess the effect of TNFα/CHX treatment on paracellular transport through the breaks in the tight junction. Control monolayers had a J_v of $3.64x10^{-6} \pm 3.73x10^{-7}$ cm/s. Fig. 3.2 shows that treatment with TNFα/CHX increased J_v by 4.31-fold. Treatment with caspase inhibitor Z-VAD-FMK significantly attenuated increase in J_v to 1.54-fold (J_v value of monolayers treated with Z-VAD-FMK at the two concentrations were not significantly different so they were combined together). The effect of TNFα/CHX and Z-VAD-FMK on water flux was totally different in BAECs monolayers. In BAECs, control monolayers had a J_v of $5.05x10^{-6} \pm 4.41x10^{-7}$ cm/s. Treatment with TNFα/CHX only increased J_v by 2.7-fold. Treatment with TNFα/CHX and Z-VAD-FMK did not significantly attenuate the increase in J_v [2].

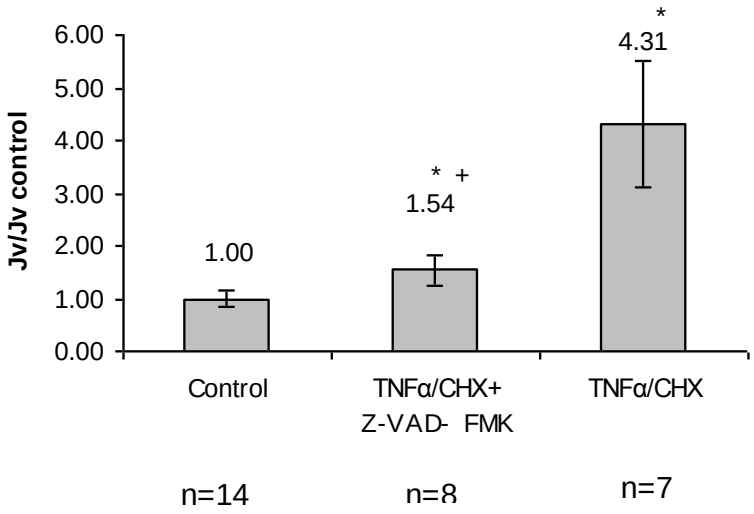

Fig 3.2 Effect of TNFα/CHX and Z-VAD-FMK on water flux (J_v). HCAEC monolayers were treated for 3 hrs and 20 mins followed by a 20-hrs recovery period. Control monolayer had an average J_v of $3.64x10^{-6} \pm 3.73x10^{-7}$ cm/s. Mean±SEM. *p<0.02 vs. control, +p<0.007 vs. TNF α/CHX.

In Cancel et al. 2010, the fact that decreasing apoptosis rate had no effect on water flux was explained by noting that previous studies [21,22,23] had shown that TNFα/CHX disrupts the junctional complex of endothelial cells independent of its apoptotic effects. In the present study, the decrease in apoptosis obtained with Z-VAD-FMK treatment did have a significant effect on water flux (Fig.3.2). This observation can be explained by the fact that, in HCAECs, a larger portion of the water transport occurs through the leaky junctions (38.5% versus 22.3% in BAECs) (Table. 2.2). In addition, there are more apoptotic cells, and therefore more leaky junctions that allow water transport, in HCAEC monolayers than in BAEC monolayers in both control monolayers (2% in HCAECs versus 0.3% in BAECs) and TNFα/CHX-treated monolayers (9.1% in HCAECs versus 5.9% in BAECs). Therefore the increase in water flux caused by TNFα/CHX treatment is a result of both a disruption of the tight junction by TNFα/CHX and an increase in individual leaky junctions resulting from increased apoptosis.

Effect of TNFα/CHX and Z-VAD-FMK on cell-cell junctions

HCAEC monolayers were immunostained for VE-cadherin to check their integrity after treatment with TNFα/CHX and Z-VAD-FMK Fig. 3.3 shows VE-cadherin staining of the monolayers after applying hydrostatic pressure. This demonstrates that there is no gross disruption on the adherens junction and that treated cells still maintain a confluent monolayer.

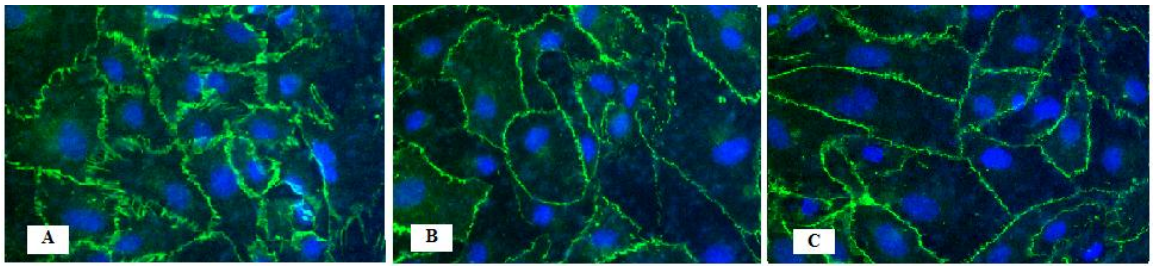

Fig. 3.3 To check the integrity of the monolayers after applying hydrostatic pressure, HCAEC were immunostained with VE-cadherin (cell junction; green) and DAPI (nuclei; blue). A) control. B) TNFa/CHX and C) TNFα/CHX+Z-VAD-FMK 25μM.

Effect of TNFα/CHX and Q-VD-OPh on apoptosis rate and LDL permeability

We used the same *in vitro* model to study the effect of another apoptosis inhibitor, Q-VD-OPh, on HCAEC monolayers. Fig. 3.4 shows the effect of TNFα/CHX and Q-VD-OPh on the apoptosis rate and convective permeability (P_e) of HCAEC monolayers to LDL. HCAEC monolayers were incubated with TNFα/CHX for 3 hours and 20 mins in the presence or absence of the inhibitor Q-VD-OPh. The baseline apoptosis was 2.0 $\pm$ 0.243%. TNFα/CHX treated monolayers had an apoptosis rate of 8.1 $\pm$ 0.959%, a 4.2-fold increase over baseline. When the cells were treated with 50 μM Q-VD-OPh and 100 μM Q-VD-OPh, the apoptosis was increased by 1.25-fold and 1.31- fold, respectively.

Control monolayers had baseline P_e of $3.32 \times 10^{-6} \pm 4.57 \times 10^{-7}$ cm/s. The permeability was raised by 3.40-fold when treated with TNFα/CHX (Fig. 3.4B). Addition

of Q-VD-OPh lowered the increase in permeability to 2.8-fold when 50μM Q-VD-OPh was added, and significantly lowered the increase in permeability to 1.7-fold when 100μM Z-VAD-FMK was added.

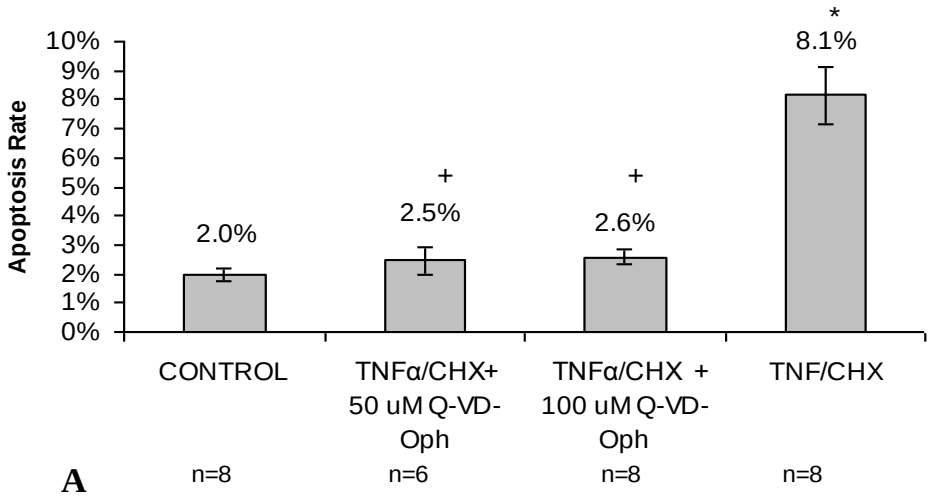

A

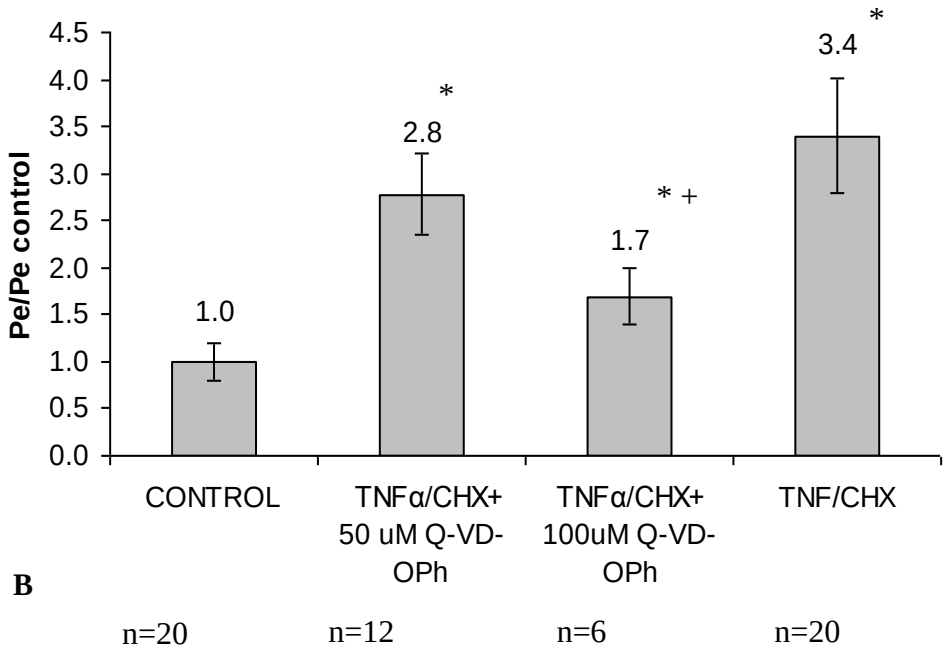

Fig 3.4 Effect of TNFα/CHX and Q-VD-Oph on (A) apoptosis rate (B) convective permeability on HCAEC monolayer. Control monolayers had an average P_e of $3.32 \times 10^{-6} \pm 4.57 \times 10^{-7}$ cm/s. Mean±SEM shown. *p<0.02 vs. control, +p<0.031 vs. TNFα/CHX.

The results for HCAECs treated with Z-VAD-FMK and Q-VD-OPh are quite similar. The apoptosis rate was raised to about 4-fold over baseline when treated with TNFα/CHX. The increase in apoptosis rate was significantly reduced when Z-VAD-FMK and Q-VD-OPh were added. The increase in permeability was also significantly reduced in HCAECs treated with Z-VAD-FMK at both 12.5 μM and 25 μM but only at 100 μM when Q-VD-OPh was used. However, it looks like a larger reduction in apoptosis leads to a smaller reduction in permeability with Q-VD-OPh.

For Z-VAD-FMK, there is no difference in apoptosis or permeability or water flux between the two concentrations. We can say that increasing in concentration of Z-VAD-FMK did not have an effect on treated monolayers.

For Q-VD-OPh, the apoptosis rates were not different between the two concentrations but the permeabilities were. This might be due to a somewhat large difference in sample sizes (n=12 for 50μM and n=6 for 100μM), or Q-VD-OPh may have other effects on the cells.

As in the previous study from our lab, we plotted the normalized LDL permeability versus the apoptosis rate to show a correlation between the two (Fig. 3.5.) The Pearson Product Moment Correlation coefficient for the Z-VAD-FMK data was calculated to be 0.70, indicating a strong correlation between LDL permeability and apoptosis (R^2=0.87). Comparing to previous study, BAECs had Pearson Product Moment Correlation of 0.72 with R^2=0.92. The larger slope in BAECs data (60.62; [2]) shows that reduction in apoptosis leads to a greater reduction in permeability, higher R^2 shows better fit of the data to a linear correlation between LDL permeability versus the apoptosis. The plot of LDL permeability versus the apoptosis rate from Q-VD-OPh data shows a similar correlation (Fig. 3.6). The Pearson Product Moment Correlation coefficient was calculated to be 0.58 (R^2=0.59) which is not a strong correlation compared to Z-VAD-FMK.

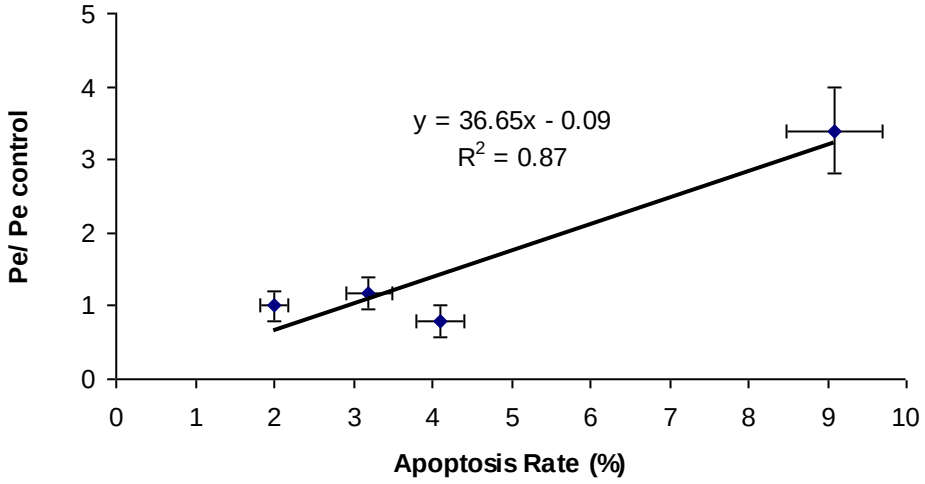

Fig 3.5 Correlation between the normalized LDL permeability and apoptosis rate of Z-VAD-FMK data, The Pearson Product Moment Correlation coefficient was calculate to be 0.70.

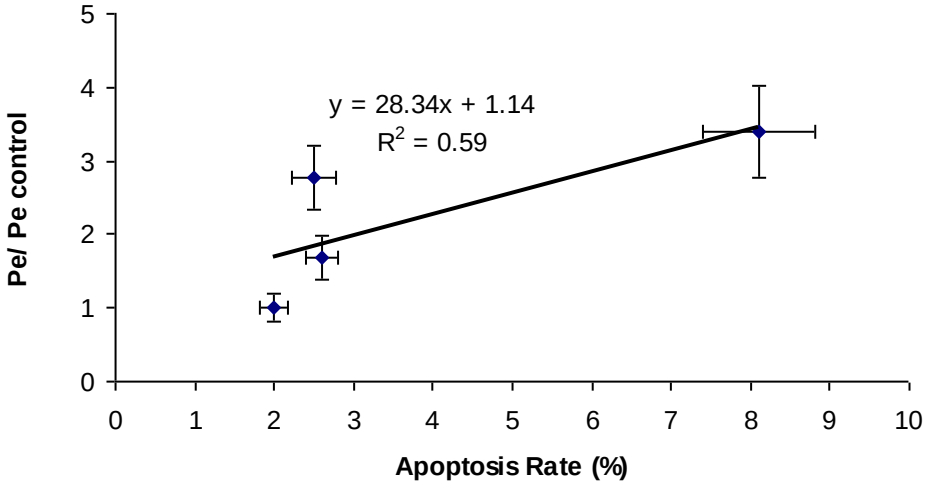

Fig 3.6 Correlation between the normalized LDL permeability and apoptosis rate of Q-VD-Oph data, The Pearson Product Moment Correlation coefficient was calculate to be 0.58.

Comparing Z-VAD-FMK with Q-VD-OPh, we see that a 3.11-fold reduction in apoptosis leads to only a 2-fold reduction in permeability with 100μM Q-VD-OPh, while a 2.2-fold reduction in apoptosis leads to a significantly higher 4.3-fold reduction in permeability with 25μM Z-VAD-FMK. This and the fact that two different

concentrations of Q-VD-OPh resulted in about the same apoptosis rate but significantly different LDL permeability leads us to believe that that Q-VD-OPh may have other effects on the cells. Future experiments include collecting more data to examine the effect of Q-VD-OPh at 100μM to eliminate the possible effect of unbalanced sample sizes. In addition more data is needed on the effect of Q-VD-OPh on water flux.

Both Z-VAD-FMK and Q-VD-OPh are irreversible caspases inhibitors. They initiate irreversible states of inhibition. Serine proteases, analogous to caspases, are involved in protein degradation during apoptosis. The roles serine proteases play in caspase-dependent versus caspases-independent cell death pathways, may help explain why cells continue to after we removed caspase inhibitors such as Z-VAD-FMK and Q-VD-OPh. Previous study showed that Cotreatment of the stressed cells with Z-VAD-FMK and the serine protease inhibitor Pefabloc (AEBSF) inhibited all typical signs of apoptosis, including phosphatidylserine (PS) exposure and the removal of apoptotic cells by phagocytosis [24]. Future experiments on co treatment of HCAECs with Z-VAD-FMK/ Q-VD-OPh and AEBSF will elucidate the roles of serine proteases in HCAECs.

The current study suggests that Z-VAD-FMK has the ability to reduce the apoptosis rate which results in a decrease in permeability of HCAEC monolayers in the same manner as BAEC under convective conditions.

References

[1] Cancel LM, Fitting A, Tarbell JM. In vitro study of LDL transport under pressurized (convective) conditions. Am J Physiol Heart Cirs physiol 293:H126-32, 2007.

[2] Cancel LM, Tarbell JM. The role of apoptosis in LDL transport through cultured endothelial cell monolayers. Atherosclerosis 208: 335-341, 2010.

[3] Schwenke DC, Carew TE. Initiation of atherosclerotic lesions in cholesterol-fed rabbits. I. Focal increases in arterial LDL concentration precede development of fatty streak lesions. Arteriosclerosis 9:895-907, 1989

[4] Schwenke DC, Carew TE. Quantification in vivo of increased LDL content and rate of LDL degradation in normal rabbit aorta occurring at sites susceptible to early atherosclerotic lesions. Circ Res. 62:699-710, 1988.

[5] Weinbaum S, Chien S. Lipid transport aspects of atherogenesis. J Biomech Eng. 115:602-10, 1993.

[6] Joseph L. Goldstein, Michael S. Brown. Receptor-mediated encocytosis : Insight from lipoprotein receptor system. Proc. Natl. Acad. Sci. USA. Vol.76, No.7, pp.3330-3337, July 1979.

[7] Ogunrinade, O., Kameya, G.T., and Truskey, G.A., "Effect of fluid shear stress on the permeability of the arterial endothelium." Ann. Biomed. Eng. 30: pp. 1-17, 2002.

[8] John M. Tarbell. Mass transport in arteries and the localization of atherosclerosis. Annu. Rev. Biomed. Eng. 5:79-118, 2003.

[9] Fu B, Curry FE, Adamson RH, Weinbaum S. A model for interpreting the tracer labeling of interendothelial clefts. Ann. Biomed. Eng. 25:375-97, 1997.

[10] Weinbaum S, Tzeghai G, Ganatos P, Pfeffer R, Chien S. Effect of cell turnover and leaky junctions on arterial macromolecular transport. Am J Physiol Heart Circ Physiol 248: H945–H958, 1985.

[11] Gerrity RG, Richardson M, Somer JB, Bell FP, Schwartz CJ. Endothelial cell morphology in areas of in vivo Evans blue uptake in the aorta of young pigs. II. Ultrastructure of the intima in areas of differing permeability to proteins. Am J Pathol 89: 313–334, 1977.

[12] Chen YL, Jan KM, Lin HS, Chien S. Ultrastructural studies on macromolecular permeability in relation to endothelial cell turnover. Artherosclerosis 118: 89-104, 1995.

[13] T Jackson. Receptor-mediated endocytosis by clathrin-coated vesicles. www.abcam.com

[14] Alberts B, Johnson A, Lewis J, et al. Molecular Biology of the Cell. 4th edition: 1010-1011, 2002

[15] Hengartner MO. The biochemistry of apoptosis. Nature 407:770–6, 2000.

[16] Ashkenazi A., Dixit V.M. Death Receptors: Signaling and Modulation. Science 281:1305-1308, 1998

[17] Li, P., Nijhawan, D., Brudihardjo, I., Srinivasula, S.M., Ahmad, M., Alnemri, E.S., and Wang, X. (1997c). Cytochrome C and dATP - dependent formation of Apaf-1/caspase-9 complex initiates an apoptotic protease cascade. Cell 91, 479–489, 1997.

[18] Luo et al. Bid, a Bcl2 interacting protein, mediates cytochrome c release from mitochondria in response to activation of cell surface death receptors. Cell 94:481-90, 1998.

[19] Kadem O, Katchalsky A. Thermodynamic analysis of the permeability of biological membranes to non-electrolytes. Biochim Biophys Acta. 27:229-46, 1958.

[20] Patlak CS, Goldstein DA & Hoffman JF. The flow of solute and solvent across a two-membrane system. J Theor Biol 5, 426–442, 1963.

[21] McKenzie JA, Ridley AJ. Roles of Rho/ROCK and MLCK in TNF-alpha-induced changes in endothelial morphology and permeability. J Cell Physiol 213:221-8, 2007.

[22] Petrache I, Birukova A, Ramirez SI, Garcia JG, Verin AD. The role of the microtubules in tumor necrosis factor-alpha-induced endothelial cell permeability. Am J Respir Cell Mol Biol 28:574-81, 2003.

[23] Wójciak-Stothard B, Entwistle A, Garg R, Ridley AJ. Regulation of TNF-alpha-induced reorganization of the actin cytoskeleton and cell-cell junctions by Rho, Rac, and Cdc42 in human endothelial cells. J Cell Physiol 176:150-65, 1998.

[24] Egger L, Schneider J, Rhême C, Tapernoux M, Häcki J, Borner C. Serine proteases mediate apoptosis-like cell death and phagocytosis under caspase-inhibiting conditions. Cell Death Differ. 10:1188-203,2003.